EFT fits to the top-quark couplings at HL-LHC and future e^+e^- colliders

Joint Workshop of the CEPC Physics, Software and New Detector Concept in 2022

24th May 2022

Víctor Miralles

in collaboration with:
Gauthier Durieux, Abel Gutiérrez Camacho, Luca Mantani, Marcos Miralles López , María Moreno Llácer, René Poncelet, Eleni Vryonidou, Marcel Vos

Based on [1907.10619], [2006.14631], [2107.13917] and [2205.02140]

Introduction

- Our goal is to constrain all the top-quark related Wilson coefficients of the SMEFT
- The fits have been performed using `HEPfit` [1910.14012]
- Estimations on the improvement of the measurements are presented for the HL-LHC
- Estimation for the relevant observables for this fit in future e^+e^- colliders are shown
- Prospects for our limits in the HL-LHC and a future e^+e^- colliders are obtained

Theoretical Framework

- We use an EFT description to parametrise deviations from the SM

Relevant Operators			
Coefficient	Operator	Coefficient	Operator
$C^1_{\varphi Q}$	$\left(\bar{Q}\gamma^\mu Q\right)\left(\varphi^\dagger i\overleftrightarrow{D}_\mu \varphi\right)$	$C^3_{\varphi Q}$	$\left(\bar{Q}\tau^I\gamma^\mu Q\right)\left(\varphi^\dagger i\overleftrightarrow{D}^I_\mu \varphi\right)$
$C_{\varphi t}$	$\left(\bar{t}\gamma^\mu t\right)\left(\varphi^\dagger i\overleftrightarrow{D}_\mu \varphi\right)$	$C_{\varphi b}$	$\left(\bar{b}\gamma^\mu b\right)\left(\varphi^\dagger i\overleftrightarrow{D}_\mu \varphi\right)$
$C_{t\varphi}$	$\left(\bar{Q}t\right)\left(\varepsilon\varphi^*\,\varphi^\dagger\varphi\right)$	C_{tG}	$\left(\bar{t}\sigma^{\mu\nu}T^A t\right)\left(\varepsilon\varphi^* G^A_{\mu\nu}\right)$
C_{tW}	$\left(\bar{Q}\tau^I\sigma^{\mu\nu}t\right)\left(\varepsilon\varphi^* W^I_{\mu\nu}\right)$	C_{tB}	$\left(\bar{Q}\sigma^{\mu\nu}t\right)\left(\varepsilon\varphi^* B_{\mu\nu}\right)$
$C^{1(ijkl)}_{qq}$	$(\bar{q}_i\gamma^\mu q_j)(\bar{q}_k\gamma_\mu q_l)$	$C^{3(ijkl)}_{qq}$	$(\bar{q}_i\tau^I\gamma^\mu q_j)(\bar{q}_k\tau^I\gamma_\mu q_l)$
$C^{(ijkl)}_{uu}$	$(\bar{u}_i\gamma^\mu u_j)(\bar{u}_k\gamma_\mu u_l)$	$C^{8(ijkl)}_{ud}$	$(\bar{u}_i\gamma^\mu T^A u_j)(\bar{d}_k\gamma_\mu T^A d_l)$
$C^{8(ijkl)}_{qu}$	$(\bar{q}_i\gamma^\mu T^A q_j)(\bar{u}_k\gamma_\mu T^A u_l)$	$C^{8(ijkl)}_{qd}$	$(\bar{q}_i\gamma^\mu T^A q_j)(\bar{d}_k\gamma_\mu T^A d_l)$
C^1_{lQ}	$\left(\bar{Q}\gamma_\mu Q\right)\left(\bar{l}\gamma^\mu l\right)$	C^3_{lQ}	$\left(\bar{Q}\tau^I\gamma_\mu Q\right)\left(\bar{l}\tau^I\gamma^\mu l\right)$
C_{lt}	$\left(\bar{t}\gamma_\mu t\right)\left(\bar{l}\gamma^\mu l\right)$	C_{lb}	$\left(\bar{b}\gamma_\mu b\right)\left(\bar{l}\gamma^\mu l\right)$
C_{eQ}	$\left(\bar{Q}\gamma_\mu Q\right)\left(\bar{e}\gamma^\mu e\right)$	C_{et}	$\left(\bar{t}\gamma_\mu t\right)\left(\bar{e}\gamma^\mu e\right)$
C_{eb}	$\left(\bar{b}\gamma_\mu b\right)\left(\bar{e}\gamma^\mu e\right)$	–	–

Theoretical Framework

- The Wilson coefficients are fitted are:

Coefficients Fitted			
2-quark	C_{tG} $C_{\varphi t}$ –	$C^3_{\varphi Q}$ $C_{\varphi b}$ $C_{t\varphi}$	$C^-_{\varphi Q} = C^1_{\varphi Q} - C^3_{\varphi Q}$ $C_{tZ} = c_W C_{tW} - s_W C_{tB}$ C_{tW}
4-quark	$C^8_{tu} = \sum_{i=1,2} 2C^{(i33i)}_{uu}$ $C^8_{Qu} = \sum_{i=1,2} C^{8(33ii)}_{qu}$ –	$C^8_{td} = \sum_{i=1,2,3} C^{8(33ii)}_{ud}$ $C^8_{Qd} = \sum_{i=1,2,3} C^{8(33ii)}_{qd}$ –	$C^{1,8}_{Qq} = \sum_{i=1,2} C^{1(i33i)}_{qq} + 3C^{3(i33i)}_{qq}$ $C^{3,8}_{Qq} = \sum_{i=1,2} C^{1(i33i)}_{qq} - C^{3(i33i)}_{qq}$ $C^8_{tq} = \sum_{i=1,2} C^{8(ii33)}_{uq}$
2-quark 2-lepton	C_{eb} C_{lb} –	C_{et} C_{lt} –	$C^+_{lQ} = C^1_{lQ} + C^3_{lQ}$ $C^-_{lQ} = C^1_{lQ} - C^3_{lQ}$ C_{eQ}

Observables from current colliders (LEP/SLC, Tevatron, LHC run 1 & 2)

- Here we show the observables included that have been measured in the actual colliders

Process	Observable	$\sqrt{s}$	$\int \mathscr{L}$	Experiment
$pp \to t\bar{t}$	$d\sigma/dm_{t\bar{t}}$ (15+3 bins)	13 TeV	140 fb^{-1}	CMS
$pp \to t\bar{t}$	$dA_C/dm_{t\bar{t}}$ (4+2 bins)	13 TeV	140 fb^{-1}	ATLAS
$pp \to t\bar{t}H + tHq$	σ	13 TeV	140 fb^{-1}	ATLAS
$pp \to t\bar{t}Z$	$d\sigma/dp_T^Z$ (7 bins)	13 TeV	140 fb^{-1}	ATLAS
$pp \to t\bar{t}\gamma$	$d\sigma/dp_T^\gamma$ (11 bins)	13 TeV	140 fb^{-1}	ATLAS
$pp \to tZq$	σ	13 TeV	77.4 fb^{-1}	CMS
$pp \to t\gamma q$	σ	13 TeV	36 fb^{-1}	CMS
$pp \to t\bar{t}W$	σ	13 TeV	36 fb^{-1}	CMS
$pp \to t\bar{b}$ (s-ch)	σ	8 TeV	20 fb^{-1}	LHC
$pp \to tW$	σ	8 TeV	20 fb^{-1}	LHC
$pp \to tq$ (t-ch)	σ	8 TeV	20 fb^{-1}	LHC
$t \to Wb$	F_0, F_L	8 TeV	20 fb^{-1}	LHC
$p\bar{p} \to t\bar{b}$ (s-ch)	σ	1.96 TeV	9.7 fb^{-1}	Tevatron
$e^-e^+ \to b\bar{b}$	R_b , A_{FBLR}^{bb}	$\sim$ 91 GeV	202.1 pb^{-1}	LEP/SLD

Observables from current colliders (LEP/SLC, Tevatron, LHC run 1 & 2)

- The measurements of $pp \to t\bar{t}$ are extremely relevant for constraining C_{tG} and the 4-fermion operators
- The measurements of $pp \to t\bar{t}H + tHq$ are needed to constrain $C_{t\varphi}$
- The helicities and $pp \to t\bar{t}\gamma$ generate important constraints on C_{tW}
- $pp \to t\bar{t}\gamma$ also provides important constraints on C_{tZ}
- $pp \to t\bar{t}Z$ generates restrictions on $C_{\varphi t}$ and C_{tZ}
- LEP observables are extremely important for $C_{\varphi b}$, $C^{-}_{\varphi Q}$ and $C^{(3)}_{\varphi Q}$
- $pp \to tZq$ becomes relevant to fully constrain the $C^{-}_{\varphi Q} - C^{(3)}_{\varphi Q}$ plane

Prospects for Measurements at HL-LHC

Theoretical Uncertainties $\longrightarrow$ scale with $1/2$

Experimental Uncertainties

- Modelling $\longrightarrow$ scale with $1/2$
- Systematic $\longrightarrow$ scale with $1/\sqrt{\mathscr{L}}$
- Statistical $\longrightarrow$ scale with $1/\sqrt{\mathscr{L}}$

Prospects for Measurements at HL-LHC

Inclusive cross sections and helicities

Process	Measured (fb)	SM (fb)	LHC Unc.					HL-LHC Unc.				
			theo.	exp.				theo.	exp.			
				stat.	sys.	mod.	tot.		stat.	sys.	mod.	tot.
$pp \to t\bar{t}H + tHq$	640	664.3	41.7	90	40	70.7	121.2	20.9	19.4	8.6	35.4	41.3
$pp \to t\bar{t}Z$	990	810.9	85.8	51.5	48.9	67.3	97.8	42.9	11.1	10.6	33.6	37.0
$pp \to t\bar{t}\gamma$	39.6	38.5	1.76	0.8	1.25	2.16	2.62	0.88	0.17	0.27	1.08	1.13
$pp \to tZq$	111	102	3.5	13.0	6.1	6.2	15.7	1.75	2.09	0.98	3.1	3.87
$pp \to t\gamma q$	115.7	81	4	17.1	21.1	21.1	34.4	2	1.9	2.3	10.6	11.0
$pp \to t\bar{t}W + \text{EW}$	770	647.5	76.1	120	59.6	73.0	152.6	38.1	13.1	6.5	36.5	39.4
$pp \to t\bar{b}$ (s-ch)	4900	5610	220	784	936	790	1454	110	35	42	395	399
$pp \to tW$	23100	22370	1570	1086	2000	2773	3587	785	49	89	1386	1390
$pp \to tq$ (t-ch)	87700	84200	250	1140	3128	4766	5810	125	51	140	2383	2390
F_0	0.693	0.687	0.005	0.009	0.006	0.009	0.014	0.003	0.0004	0.0003	0.004	0.004
F_L	0.315	0.311	0.005	0.006	0.003	0.008	0.011	0.003	0.0003	0.0002	0.004	0.004

Measurements at e^+e^- colliders: b-quark observables

Machine	Polarisation	Energy	Luminosity	Observable
ILC	P(e^+, e^-):(-30%, $+80\%$) P(e^+, e^-):($+30\%$, -80%)	250 GeV	2 ab^{-1}	$\sigma_{b\bar{b}}$ $A_{\text{FB}}^{b\bar{b}}$
		500 GeV	4 ab^{-1}	
		1 TeV	8 ab^{-1}	
CLIC	P(e^+, e^-):(0%, $+80\%$) P(e^+, e^-):(0%, -80%)	380 GeV	2 ab^{-1}	$\sigma_{b\bar{b}}$ $A_{\text{FB}}^{b\bar{b}}$
		1.5 TeV	2.5 ab^{-1}	
		3 TeV	5 ab^{-1}	
CEPC/FCC-ee	Unpolarised	Z-pole	57.5/150 ab^{-1}	$\sigma_{b\bar{b}}$ $A_{\text{FB}}^{b\bar{b}}$
		240 GeV	20/5 ab^{-1}	
		360/365 GeV	1/1.5 ab^{-1}	

- These observables set constraints on the EW precision observables $C_{\varphi Q}^{+} = C_{\varphi Q}^{1} + C_{\varphi Q}^{3}$ and $C_{\varphi b}$
- Also relevant for 2-quark 2-lepton operators C_{lQ}^{+}, C_{lb} and C_{eb}
- The higher-energy measurement are more relevant for the 2-quark 2-lepton operators

Measurements at e^+e^- colliders: t-quark observables

Machine	Polarisation	Energy	Luminosity	Observable
ILC	P(e^+, e^-):(-30%, $+80\%$)	500 GeV	4 ab^{-1}	Optimal Observables
	P(e^+, e^-):($+30\%$, -80%)	1 TeV	8 ab^{-1}	
CLIC	P(e^+, e^-):(0%, $+80\%$)	380 GeV	2 ab^{-1}	Optimal Observables
	P(e^+, e^-):(0%, -80%)	1.5 TeV	2.5 ab^{-1}	
		3 TeV	5 ab^{-1}	
CEPC/FCC-ee	Unpolarised	350 GeV	0.2 ab^{-1}	Optimal Observables
		365 GeV	1/1.5 ab^{-1}	

- Optimal observables maximally exploit the information in the fully differential $e^+e^- \to t\bar{t} \to bW^+\bar{b}W^-$ distribution [1807.02121]
- These constrain the 2-fermion operators $C^-_{\varphi Q}$, $C_{\varphi t}$, C_{tW} and C_{tZ}
- Also the 2-quark 2-lepton operators C^-_{lQ}, C_{lt}, C_{et} and C_{eQ}
- With these we eliminate blind directions in the $C^{(1)}_{\varphi Q} - C^{(3)}_{\varphi Q}$ plane
- Two different energies above the $t\bar{t}$ threshold are need to constrain all the 2- and 4-fermion operators

HL-LHC

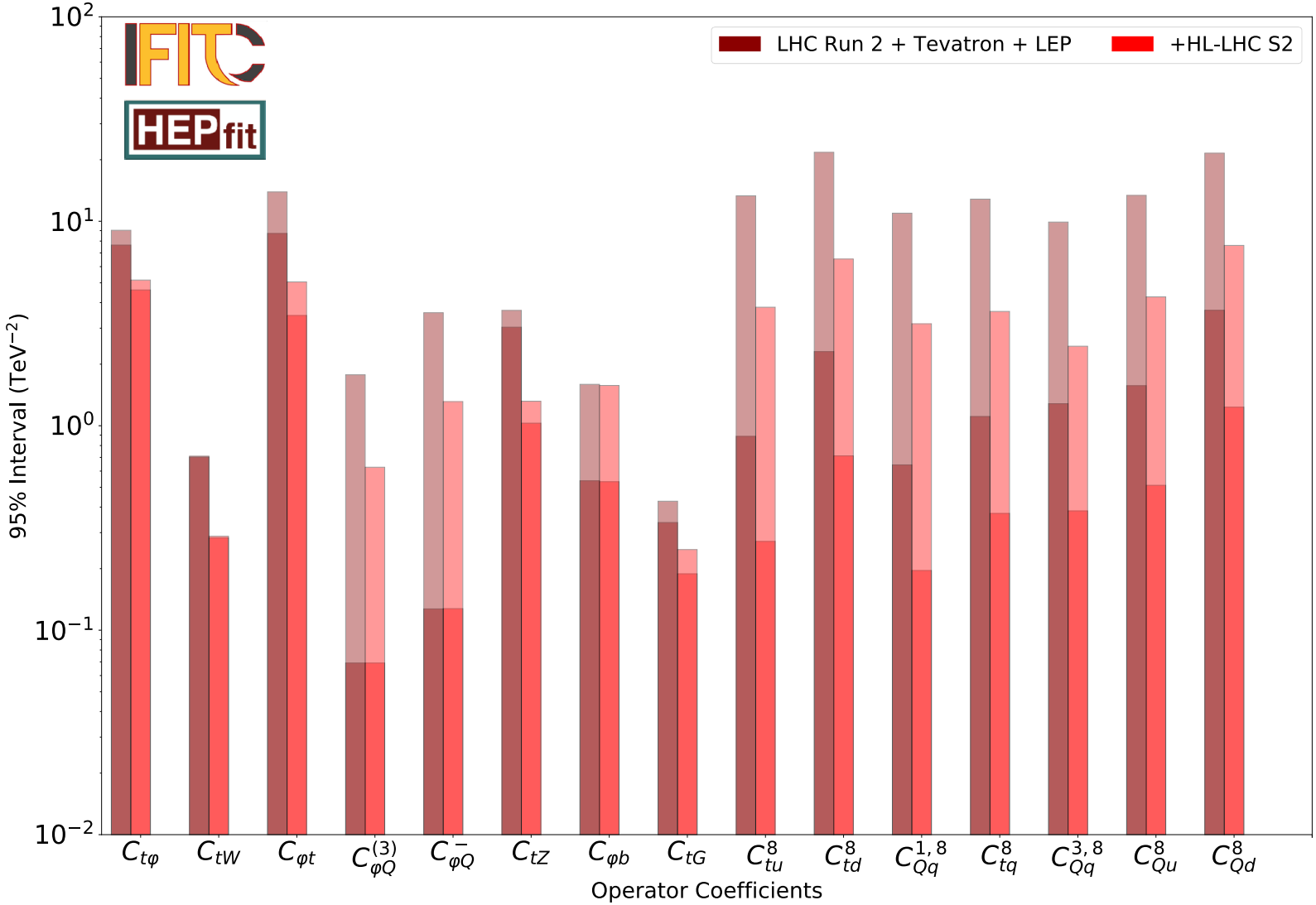
IFIC
HEPfit
LHC Run 2 + Tevatron + LEP
+HL-LHC S2
95% Interval (TeV^{-2})
10^{2}
10^{1}
10^{0}
10^{-1}
10^{-2}
$C_{t\varphi}$
C_{tW}
$C_{\varphi t}$
$C_{\varphi Q}^{(3)}$
$C_{\varphi Q}^{-}$
C_{tZ}
$C_{\varphi b}$
C_{tG}
C_{tu}^{8}
C_{td}^{8}
$C_{Qq}^{1,8}$
C_{tq}^{8}
$C_{Qq}^{3,8}$
C_{Qu}^{8}
C_{Qd}^{8}
Operator Coefficients

HL-LHC and ILC results

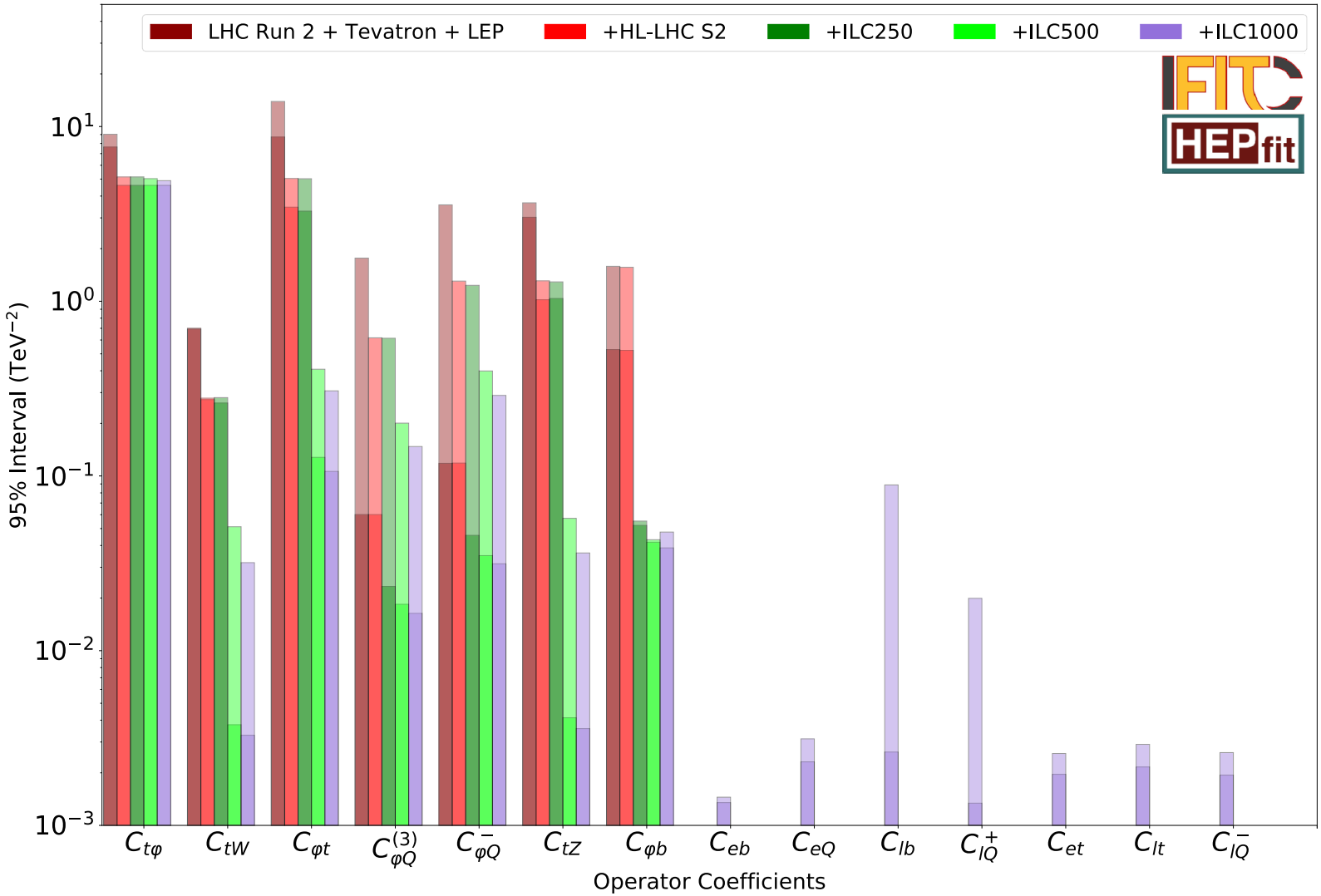

Comparison of future colliders

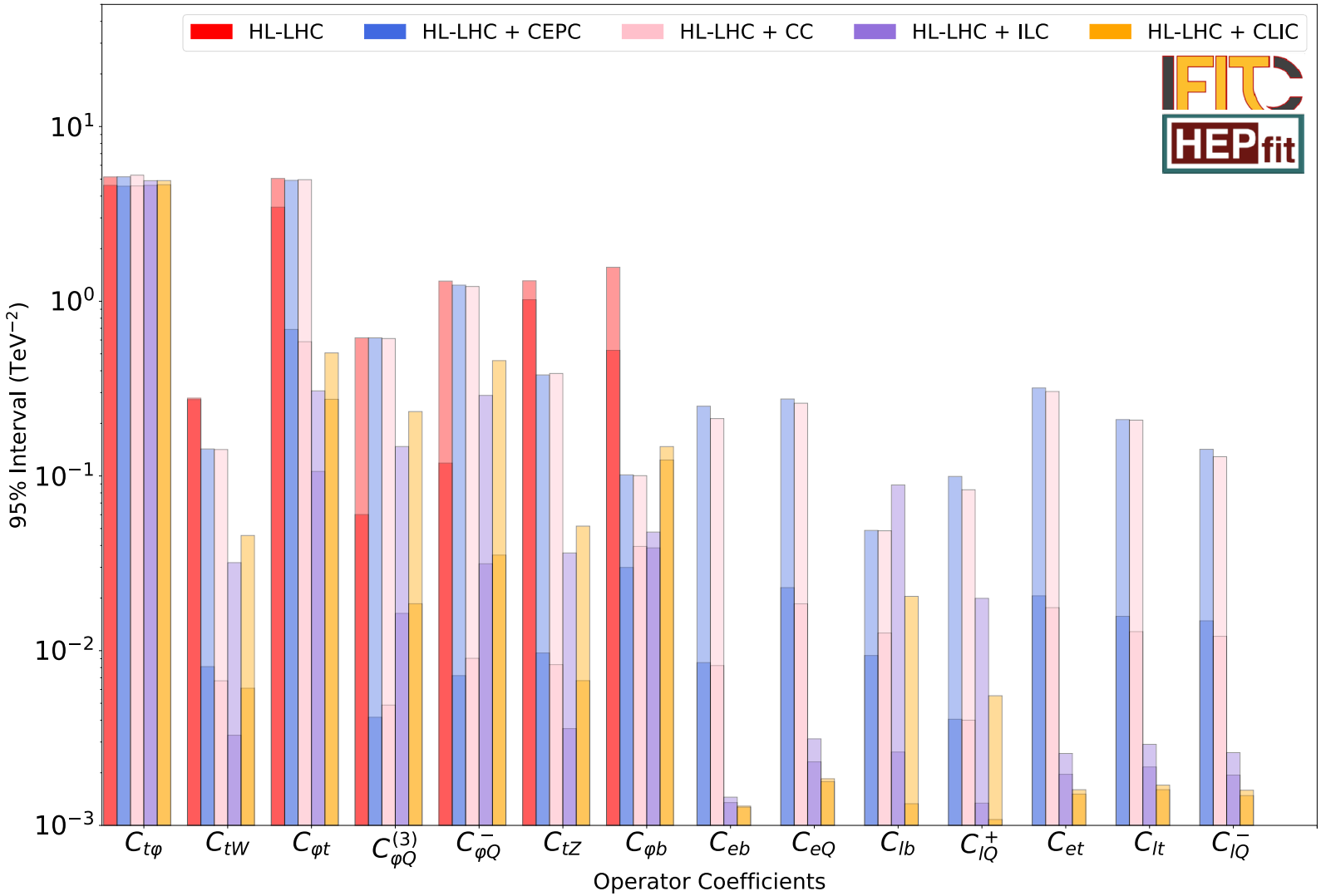

Summary

- HL-LHC expected to improve the bounds by roughly a factor 3 w.r.t. current state-of-the-art LHC run 2 + Tevatron + LEP/SLC
- An e^+e^- collider can significantly improve bounds on bottom-quark operators, and on top-quark operators if operated above the $t\bar{t}$ threshold
- Circular colliders (FCC-*ee* and CECP) operated at and slightly above the $t\bar{t}$ threshold can improve bottom- and top- operators by factor 5 and 2 for 2-fermion operators.
- Very competitive bounds on 2F bottom-operator coefficients from TeraZ
- Power to constrain 4-fermion operators limited by energy reach
- Linear colliders (ILC and CLIC) operated at two center-of-mass energies above the $t\bar{t}$ threshold can provide very tight bounds on all operators, with bounds on 4F taking advantage of energy-growing sensitivity

Thank you!

Back up

Sensitivity

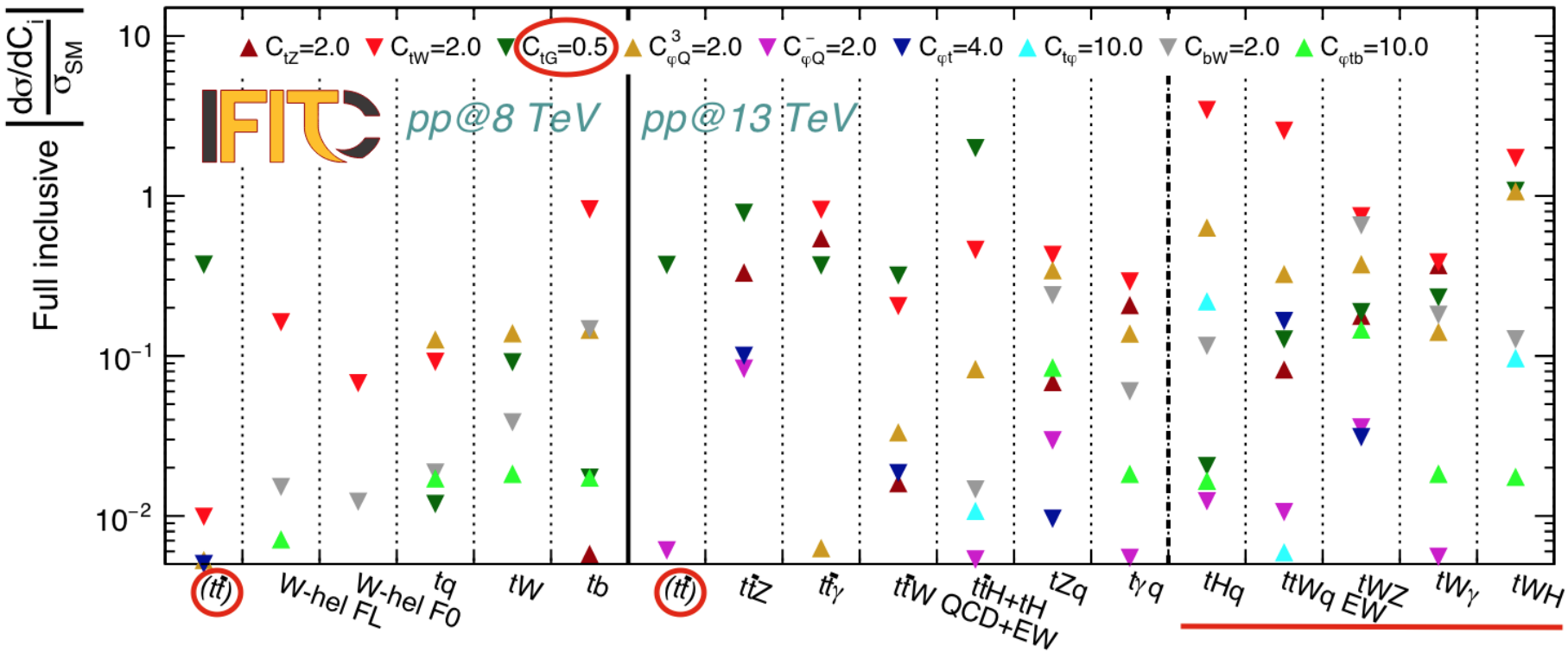

Future Colliders - Prospects for Measurements at HL-LHC

$pp \to t\bar{t}Z$ differential cross section

$pp \to t\bar{t}Z$	Measured ($\text{fb}\cdot\text{GeV}^{-1}$)	SM ($\text{fb}\cdot\text{GeV}^{-1}$)	LHC Unc.					HL-LHC Unc.				
			theo.	exp.				theo.	exp.			
				stat.	sys.	mod.	tot.		stat.	sys.	mod.	tot.
p_T^Z : (0-40)	1.47	2.21	0.263	0.53	0.23	0.21	0.615	0.132	0.114	0.050	0.105	0.163
p_T^Z : (40-70)	4.32	4.59	0.543	0.94	0.60	0.51	1.223	0.272	0.203	0.130	0.253	0.349
p_T^Z : (70-110)	4.24	4.60	0.555	0.75	0.54	0.36	0.993	0.278	0.162	0.117	0.182	0.270
p_T^Z : (110-160)	4.4	3.45	0.429	0.55	0.43	0.39	0.800	0.215	0.118	0.093	0.197	0.248
p_T^Z : (160-220)	1.75	2.05	0.261	0.31	0.15	0.13	0.371	0.131	0.067	0.033	0.066	0.100
p_T^Z : (220-290)	0.58	1.03	0.130	0.16	0.047	0.034	0.174	0.065	0.035	0.010	0.017	0.041
p_T^Z : (290-400)	0.56	0.59	0.071	0.11	0.055	0.057	0.132	0.036	0.023	0.012	0.029	0.038

Table: We show the unfolded bin contents for the absolute parton-level differential cross-section measurement.

Future Colliders - Prospects for Measurements at HL-LHC

$pp \to t\bar{t}\gamma$ differential cross section

$pp \to t\bar{t}\gamma$	Measured (fb · GeV^{-1})	SM (fb · GeV^{-1})	LHC Unc.					HL-LHC Unc.				
			theo.	exp.				theo.	exp.			
				stat.	sys.	mod.	tot.		stat.	sys.	mod.	tot.
p_T^γ : (20-25)	1.782	1.670	0.066	0.116	0.168	0.108	0.231	0.033	0.025	0.036	0.054	0.070
p_T^γ : (25-30)	1.328	1.183	0.040	0.089	0.052	0.092	0.138	0.020	0.019	0.011	0.046	0.051
p_T^γ : (30-35)	0.966	0.8663	0.0302	0.072	0.026	0.060	0.097	0.0151	0.016	0.0056	0.030	0.0342
p_T^γ : (35-40)	0.705	0.6616	0.0205	0.058	0.015	0.042	0.0733	0.0103	0.0125	0.0032	0.021	0.0248
p_T^γ : (40-47)	0.474	0.4790	0.0160	0.04	0.0096	0.048	0.0629	0.0080	0.0086	0.0021	0.024	0.0254
p_T^γ : (47-55)	0.333	0.3464	0.0094	0.031	0.0067	0.017	0.0360	0.0047	0.0067	0.0014	0.0085	0.0109
p_T^γ : (55-70)	0.221	0.2188	0.0056	0.019	0.0038	0.0081	0.0210	0.0028	0.0041	0.00082	0.0041	0.0058
p_T^γ : (70-85)	0.122	0.1286	0.0031	0.014	0.0026	0.0069	0.0158	0.0016	0.0030	0.00056	0.0035	0.0046
p_T^γ : (85-132)	0.060	0.06037	0.0017	0.005	0.0014	0.0068	0.0086	0.00084	0.0011	0.00029	0.0034	0.0036
p_T^γ : (132-180)	0.020	0.02373	0.00077	0.003	0.00044	0.00080	0.00314	0.00039	0.00065	0.000095	0.00040	0.00077
p_T^γ : (180-300)	0.009	0.00790	0.00028	0.00045	0.000085	0.0014	0.00144	0.00014	0.000097	0.000018	0.00068	0.00069

Table: We show the unfolded bin contents for the absolute parton-level differential cross-section measurement.

Future Colliders - Complementarity on e^+e^- Colliders

Good complementarity between $b\bar{b}$ (LEP) and $t\bar{t}$ (future e^+e^- collider) if we reach $\sqrt{s} > 2m_t$

$$\delta g_L^t = -(C_{\varphi Q}^1 - C_{\varphi Q}^3) m_t^2/\Lambda^2$$

$$\delta g_L^b = -(C_{\varphi Q}^1 + C_{\varphi Q}^3) m_t^2/\Lambda^2$$

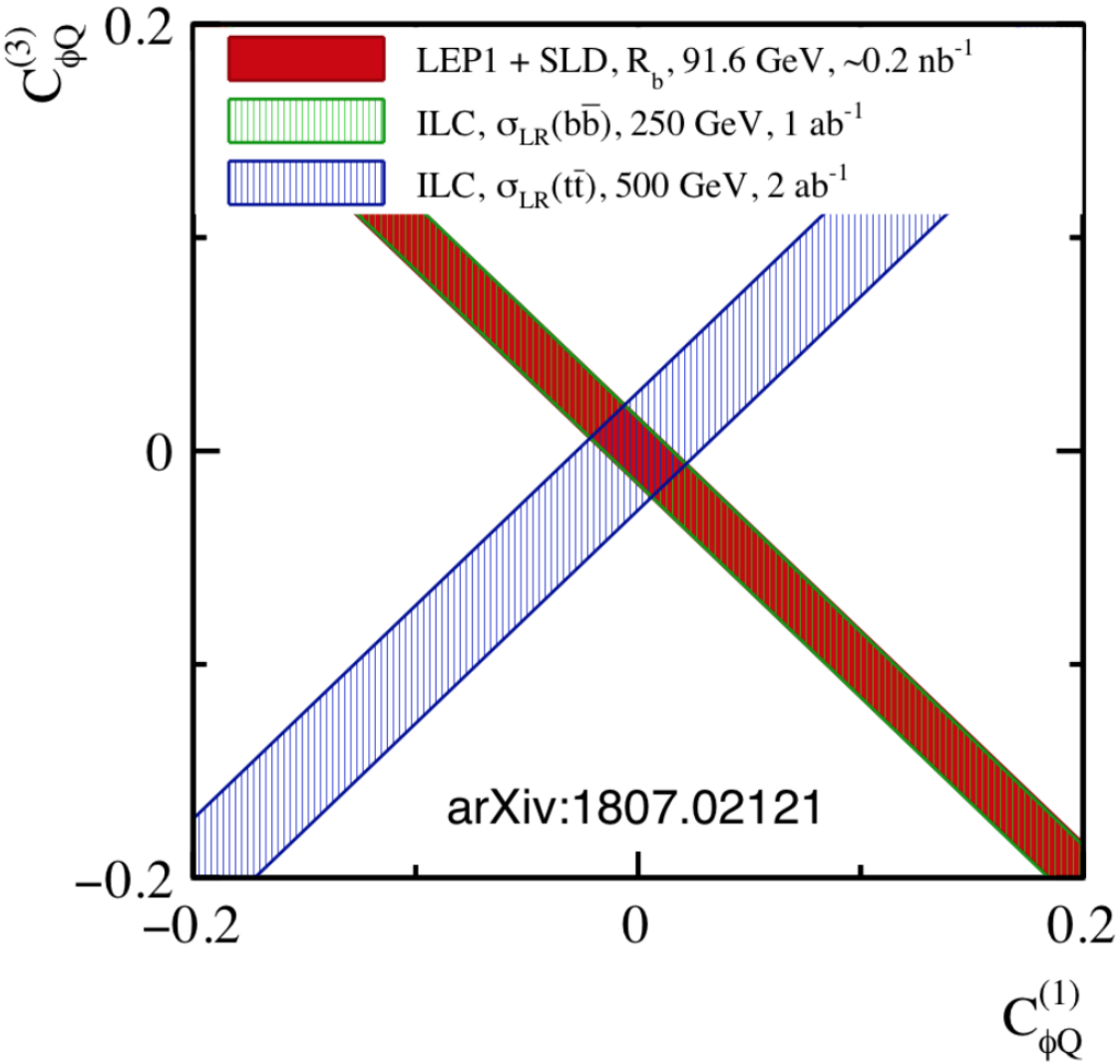

Results - Differential Cross Section Effect

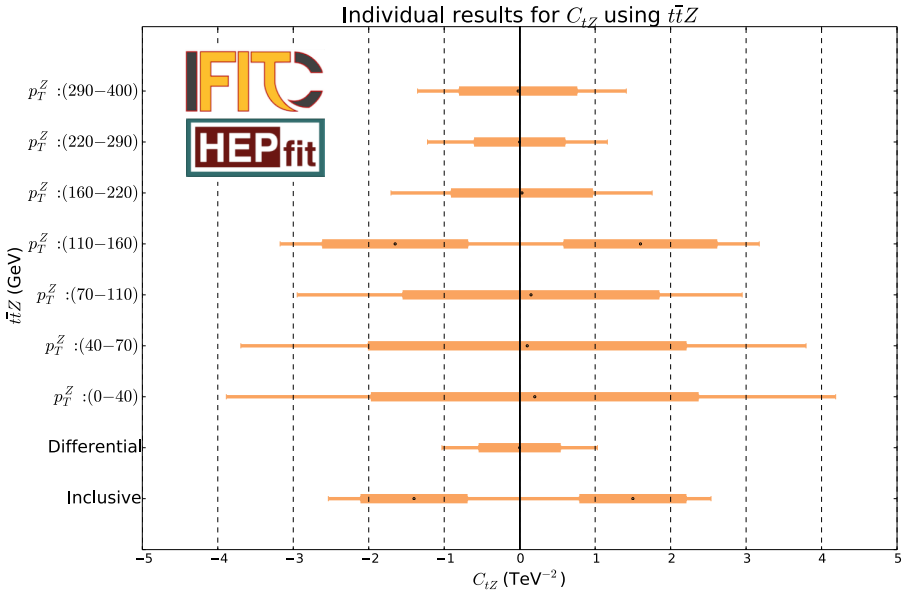

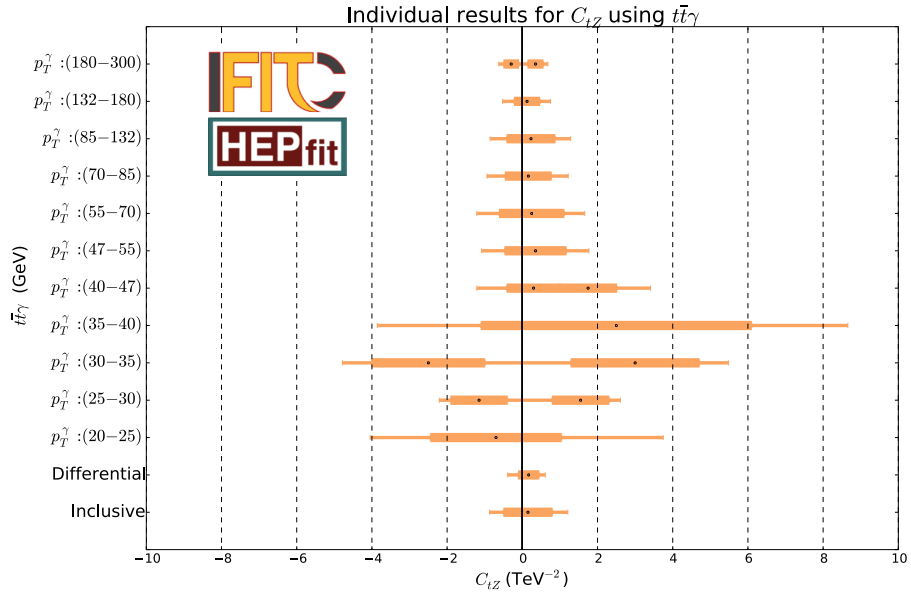

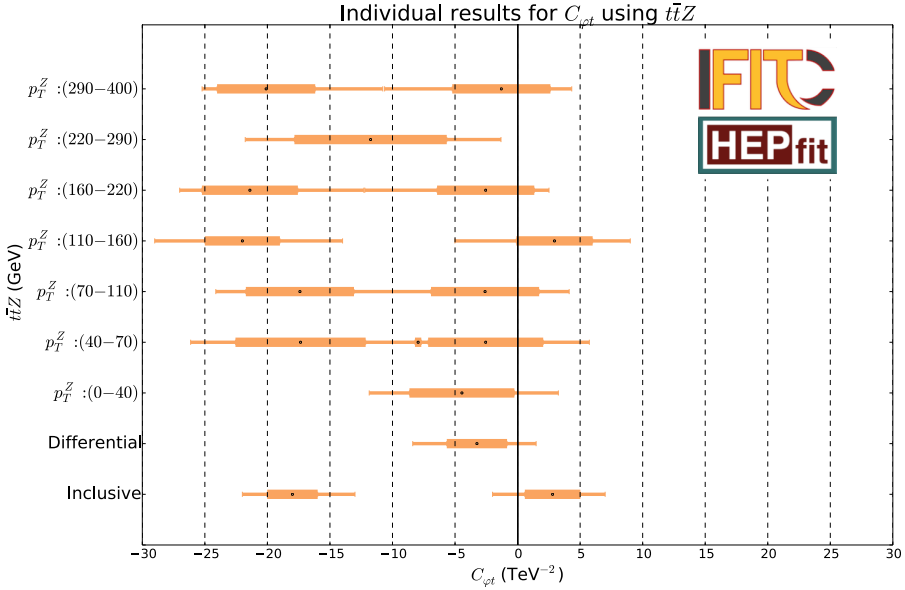

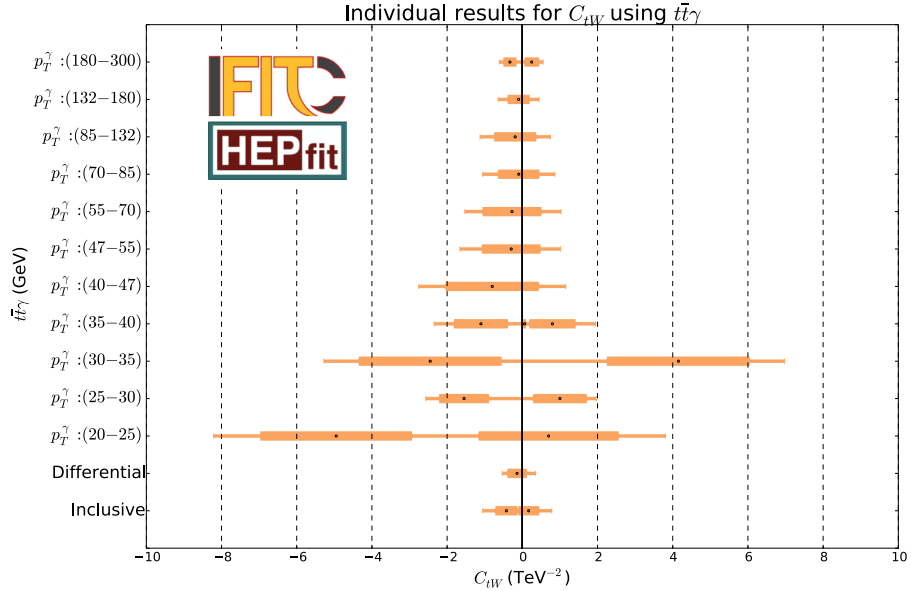

Results - Complementarity Between Observables

- Very good complementarity between the observables
- The data set is diverse enough to avoid the existence of blind directions

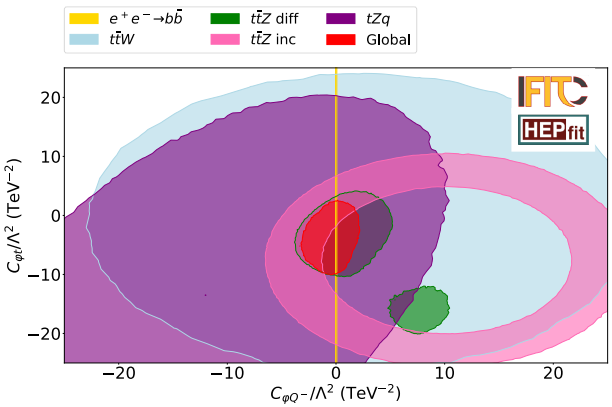

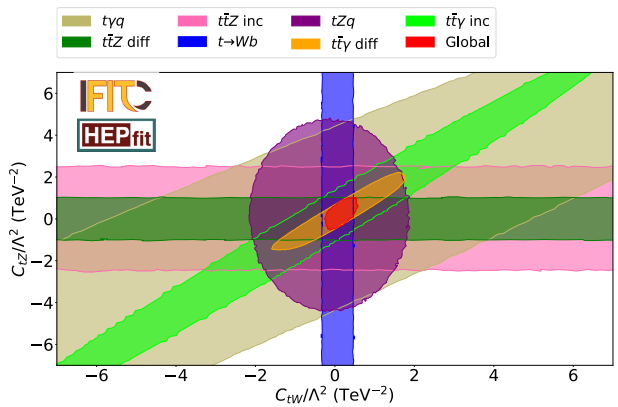

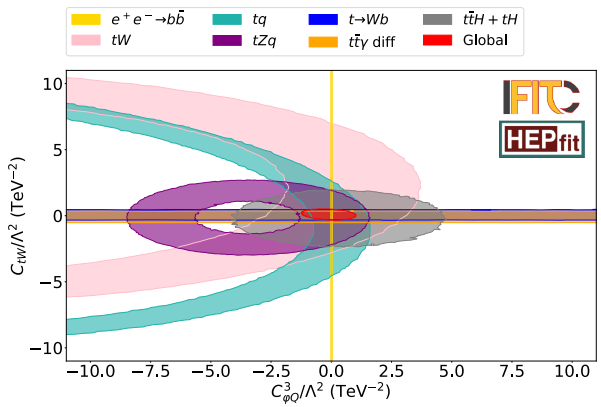

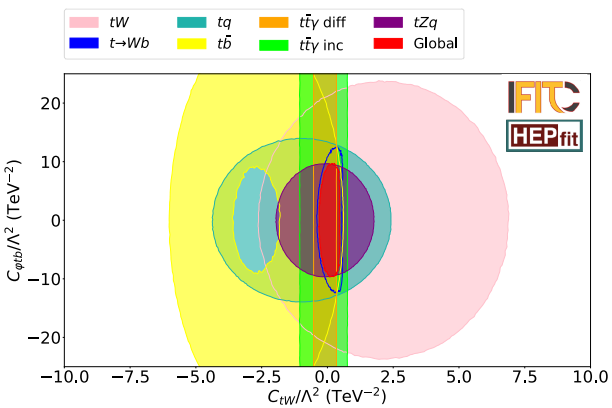

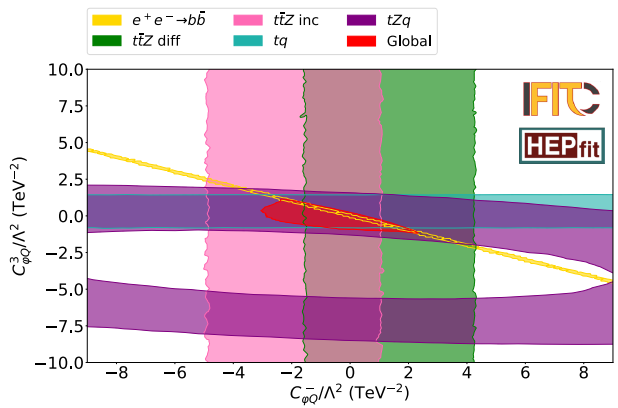

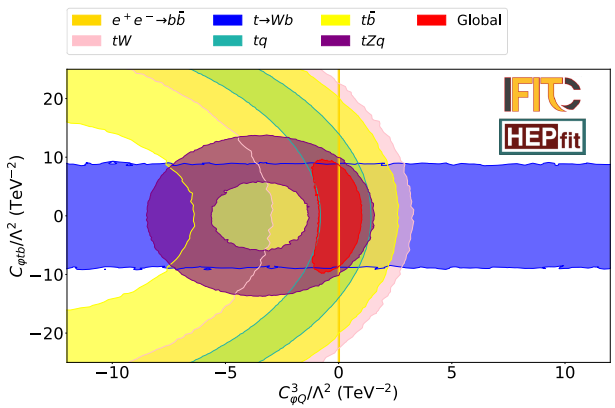

Dependencies

[1910.03606]

parameter	$t\bar{t}$	single t	tW	tZ	t decay	$t\bar{t}Z$	$t\bar{t}W$
$C_{Qq}^{1,8}$	Λ^{-2}	–	–	–	–	Λ^{-2}	Λ^{-2}
$C_{Qq}^{3,8}$	Λ^{-2}	Λ^{-4} $[\Lambda^{-2}]$	–	Λ^{-4} $[\Lambda^{-2}]$	Λ^{-4} $[\Lambda^{-2}]$	Λ^{-2}	Λ^{-2}
C_{tu}^{8}, C_{td}^{8}	Λ^{-2}	–	–	–	–	Λ^{-2}	–
$C_{Qq}^{1,1}$	Λ^{-4} $[\Lambda^{-2}]$	–	–	–	–	Λ^{-4} $[\Lambda^{-2}]$	Λ^{-4} $[\Lambda^{-2}]$
$C_{Qq}^{3,1}$	Λ^{-4} $[\Lambda^{-2}]$	Λ^{-2}	–	Λ^{-2}	Λ^{-2}	Λ^{-4} $[\Lambda^{-2}]$	Λ^{-4} $[\Lambda^{-2}]$
C_{tu}^{1}, C_{td}^{1}	Λ^{-4} $[\Lambda^{-2}]$	–	–	–	–	Λ^{-4} $[\Lambda^{-2}]$	–
C_{Qu}^{8}, C_{Qd}^{8}	Λ^{-2}	–	–	–	–	Λ^{-2}	–
C_{tq}^{8}	Λ^{-2}	–	–	–	–	Λ^{-2}	Λ^{-2}
C_{Qu}^{1}, C_{Qd}^{1}	Λ^{-4} $[\Lambda^{-2}]$	–	–	–	–	Λ^{-4} $[\Lambda^{-2}]$	–
C_{tq}^{1}	Λ^{-4} $[\Lambda^{-2}]$	–	–	–	–	Λ^{-4} $[\Lambda^{-2}]$	Λ^{-4} $[\Lambda^{-2}]$
$C_{\phi Q}^{-}$	–	–	–	Λ^{-2}	–	Λ^{-2}	–
$C_{\phi Q}^{3}$	–	Λ^{-2}	Λ^{-2}	Λ^{-2}	Λ^{-2}	–	–
$C_{\phi t}$	–	–	–	Λ^{-2}	–	Λ^{-2}	–
$C_{\phi tb}$	–	Λ^{-4}	Λ^{-4}	Λ^{-4}	Λ^{-4}	–	–
C_{tZ}	–	–	–	Λ^{-2}	–	Λ^{-2}	–
C_{tW}	–	Λ^{-2}	Λ^{-2}	Λ^{-2}	Λ^{-2}	–	–
C_{bW}	–	Λ^{-4}	Λ^{-4}	Λ^{-4}	Λ^{-4}	–	–
C_{tG}	Λ^{-2}	$[\Lambda^{-2}]$	Λ^{-2}	–	$[\Lambda^{-2}]$	Λ^{-2}	Λ^{-2}

Table 1. Wilson coefficients in our analysis and their contributions to top-quark observables via SM-interference (Λ^{-2}) and via dimension-6 squared terms only (Λ^{-4}). A square bracket indicates that the Wilson coefficient contributes via SM-interference at NLO QCD. All quark masses except m_t are assumed to be zero. 'Single t' stands for $s-$ and $t-$channel electroweak top production.

Measurements at e^+e^- colliders: b-quark observables

Machine	Polarisation	Energy	Luminosity	Observable	Value
ILC	P(e^+, e^-):(-30%, $+80\%$)	250 GeV	2 ab^{-1}	σ_b	3182 ± 4.930 fb
				A_{FB}^b	0.6267 ± 0.000738
		500 GeV	4 ab^{-1}	σ_b	693.5 ± 1.188 fb
				A_{FB}^b	0.6194 ± 0.001140
		1 TeV	8 ab^{-1}	σ_b	168.10 ± 0.311 fb
				A_{FB}^b	0.617 ± 0.001342
	P(e^+, e^-):($+30\%$, -80%)	250 GeV	2 ab^{-1}	σ_b	960.6 ± 1.774 fb
				A_{FB}^b	0.426 ± 0.00201
		500 GeV	4 ab^{-1}	σ_b	203.9 ± 0.442 fb
				A_{FB}^b	0.493 ± 0.00268
		1 TeV	8 ab^{-1}	σ_b	49.21 ± 0.145
				A_{FB}^b	0.507 ± 0.00335
CLIC	P(e^+, e^-):(0%, $+80\%$)	380 GeV	1 ab^{-1}	σ_b	964.6 ± 2.03 fb
				A_{FB}^b	0.680 ± 0.002
		1.5 TeV	2.5 ab^{-1}	σ_b	57.8 ± 0.311 fb
				A_{FB}^b	0.674 ± 0.005
		3 TeV	5 ab^{-1}	σ_b	14.41 ± 0.0923 fb
				A_{FB}^b	0.673 ± 0.008
	P(e^+, e^-):(0%, -80%)	380 GeV	1 ab^{-1}	σ_b	329.8 ± 1.01 fb
				A_{FB}^b	0.479 ± 0.004
		1.5 TeV	2.5 ab^{-1}	σ_b	19.61 ± 0.153 fb
				A_{FB}^b	0.520 ± 0.011
		3 TeV	5 ab^{-1}	σ_b	4.88 ± 0.0505
				A_{FB}^b	0.522 ± 0.015
FCC	Unpolaried	Z-pole	150 ab^{-1}	σ_b	8340800 ± 2449 fb
				A_{FB}^b	0.23365 ± 0.000130
		240 GeV	5 ab^{-1}	σ_b	1670 ± 2.51 fb
				A_{FB}^b	0.584 ± 0.000679
		365 GeV	1.5 ab^{-1}	σ_b	647.2 ± 1.341 fb
				A_{FB}^b	0.591 ± 0.0016
CEPC	Unpolaried	Z-pole	57.5 ab^{-1}	σ_b	8340800 ± 1947 fb
				A_{FB}^b	0.23365 ± 0.000130
		240 GeV	20 ab^{-1}	σ_b	1670 ± 2.40 fb
				A_{FB}^b	0.584 ± 0.000339
		365 GeV	1 ab^{-1}	σ_b	647.2 ± 1.51 fb
				A_{FB}^b	0.591 ± 0.00200